

## P-Glycoprotein Substrates and Antagonists Cluster into Two Distinct Groups

STEFANIA SCALA, NADIA AKHMED, U. S. RAO, KEN PAULL, LU-BIN LAN, BRUCE DICKSTEIN, JONG-SEOK LEE, GALAL H. ELGEMEIE, WILFRED D. STEIN, and SUSAN E. BATES

Medicine Branch, Division of Clinical Sciences (S.S., N.A., B.D., S.E.B.), and Information Technology Branch, Division of Basic Sciences (K.P.), National Cancer Institute, National Institutes of Health, Bethesda, Maryland, Department of Pharmacology, University of North Carolina, Chapel Hill, North Carolina (U.S.R.), Silberman Institute of Life Sciences, Hebrew University, Jerusalem, Israel (L.-B.L., W.D.S.), Department of Internal Medicine, Gyeongsang National University, Kyungnam, South Korea (J.-S.L.) and Helwan University, Cairo, Egypt (G.H.E.)

Received June 20, 1996; Accepted February 25, 1997

### SUMMARY

To gather further insight into the interaction between P-glycoprotein (Pgp) and its substrates, 167 compounds were analyzed in multidrug resistant human colon carcinoma cells. These compounds were selected from the National Cancer Institute Drug Screen repository using computer-generated correlations with known Pgp substrates and antagonists. The compounds were prospectively defined as Pgp substrates if cytotoxicity was increased  $\geq 4$ -fold by the addition of cyclosporin A (CsA) and as Pgp antagonists if inhibition of efflux increased rhodamine accumulation by 4-fold. Among the 84 agents that met either criterion, 35 met only the criterion for substrates, 42 met only the criterion for antagonists, and only

seven met both criteria. Thus, compounds interacting with Pgp form two distinct groups: one comprising cytotoxic compounds that are transported and have poor or no antagonistic activity and a second comprising compounds with antagonistic activity and no evidence of significant transport. Vinblastine accumulation and kinetic studies performed on a subset of 18 compounds similarly differentiated substrates and antagonists, but inhibition of  $^3\text{H}$ -azidopine labeling and induction of ATPase activity did not. These data support an emerging concept of Pgp in which multiple regions instead of specific sites are involved in drug transport.

The overexpression of Pgp, product of the *MDR-1* gene, results in a well-characterized mechanism of chemoresistance known as multidrug resistance (1). Pgp is a 170-kDa membrane glycoprotein with two consensus sequences for ATP binding that functions as an energy-dependent drug efflux pump (1). In laboratory models, overexpression of Pgp can confer resistance to structurally dissimilar groups of antineoplastic agents, including vinblastine, doxorubicin, and paclitaxel. Pgp expression is found in a number of normal human and other mammalian tissues (2). Although *in vitro* studies suggest interaction of the transporter with progesterone and cyclic and linear peptides (3–7), the physiological substrates, sites, and mechanisms of drug binding to Pgp have not yet been identified.

Among the compounds interacting with Pgp, several drugs have been identified as chemosensitizers, which are able to restore sensitivity to cytotoxic agents by inhibiting the transport of Pgp substrates. These Pgp antagonists include calcium channel antagonists, antiarrhythmics, antihypertensives, diterpenes, cyclosporines, and many others (1). However, interactions between Pgp and its transported substrates, or its antagonists, have not been fully understood. It has been widely thought that Pgp antagonism occurs through

competition with substrates for drug transport (8, 9). Emerging evidence suggests that there are different categories of substrates due to multiple binding sites or to a complex binding site with different regions of interaction (10–15).

It has been suggested that Pgp antagonists fall into two groups: those that are transported themselves and those that are not (16). Verapamil and CsA are in the first group, whereas progesterone is found in the latter group (17–19). Our laboratory studies suggested, however, that when transport increased for a compound, its antagonistic potency declined (20, 21), and that overall, the transport of Pgp antagonists is quite poor.

In an attempt to improve our understanding of the interaction of Pgp with its substrates, we studied 120 individual compounds selected from the National Cancer Institute Drug Screen database and an additional 47 analogues of an antagonist identified early in the study. These compounds were chosen through the use of COMPARE, a computer-based pattern identification program that evaluates patterns of cytotoxicity of compounds analyzed in the cell lines of the drug screen. The program gives a correlation coefficient for the degree of similarity between patterns of cytotoxicity, which helps to identify compounds with similar targets,

**ABBREVIATIONS:** Pgp, P-glycoprotein; CsA, cyclosporin A; DMF, dose-modifying factor.

mechanisms of action, and mechanisms of resistance (22). The compounds were chosen on the basis of high correlations coefficients with known Pgp substrates and antagonists. In the latter case, compounds highly correlated with verapamil, quinidine, cyclosporin A, amiodarone, and quinine were chosen for study. Although previous studies had shown that compounds highly correlated with Pgp substrates were likely to be well transported themselves (23, 24), the same was not known for compounds highly correlated with Pgp antagonists. We characterized the selected compounds for their ability to be transported by Pgp and to antagonize Pgp-mediated transport.

## Experimental Procedures

**Materials.** The 167 test compounds evaluated as Pgp substrates and antagonists were provided by the Drug Synthesis and Chemistry Branch, National Cancer Institute Drug Screen Program. Verapamil and CsA were from Sigma Chemical (St. Louis, MO). PSC 833 was from Novartis Pharmaceuticals (East Hanover, NJ).

**Cell lines.** SW620 Ad300 is a multidrug-resistant human colon carcinoma subline that was selected from parental SW620 cells and maintained in 300 ng/ml doxorubicin. SW620 Ad300 cells are carried in RPMI, 10% fetal calf serum, penicillin, streptomycin, and glutamine. SW620 Ad300 cells possess a multidrug-resistant phenotype and do not seem to have mechanisms of resistance other than over-expression of Pgp (25).

**National Cancer Institute Drug Screen database.** The National Cancer Institute Drug Screen database contains information on >48,000 compounds characterized for cytotoxicity patterns in 60 human cancer cell lines (22). The differing sensitivities of each of the 60 cell lines for each compound define a pattern of cytotoxicity, which is displayed as a "fingerprint" when the  $IC_{50}$  values are plotted. The computer program COMPARE determines the correlation between a compound of interest and each compound in the database, ranking them by correlation coefficient. High correlation coefficients are obtained between compounds with similar cytotoxicity profiles, even if they are not structurally similar (22, 26). We recently demonstrated that Pgp substrates could be identified by COMPARE through correlation of the cytotoxicity profiles with the profile obtained by MDR-1 mRNA measurement or by a functional assay for Pgp with the use of rhodamine 123 (23, 24). Compounds with high Pearson correlation coefficients are likely to be Pgp substrates. We used COMPARE to select compounds with high correlation coefficients with either known Pgp substrates or known Pgp antagonists. Because Pgp substrates are readily identified and represented in large numbers in the National Cancer Institute Drug Screen (23, 24), we made a special effort to identify compounds correlating with antagonists. In addition, we studied 47 structural analogues of the best antagonist identified (NSC 667739). Finally, in an attempt to find more compounds meeting the criteria for both substrate and antagonist, a modified version of COMPARE was used to select compounds correlating with the seven compounds meeting the criteria for both substrate and antagonist. In all, 167 compounds were studied, including four well-known Pgp substrates and three well-known Pgp antagonists. Compounds were resuspended in dimethylsulfoxide, a diluent that demonstrated no interaction with Pgp at the concentrations used in the assays (<1%).

**Rhodamine 123 efflux.** Assays were carried out as previously described (23). Suspensions of logarithmic phase cells were obtained from tissue culture plates by trypsinization. During the accumulation period, 100  $\mu$ l of cell suspension was resuspended in rhodamine-containing medium (phenol red-free improved minimum essential medium plus 10% fetal bovine serum containing 0.5  $\mu$ g/ml rhodamine) and incubated with or without 3  $\mu$ g/ml CsA or 1, 10, and 100  $\mu$ M concentration of the test compound at 37° in 5% CO<sub>2</sub> for 30 min. After the accumulation period, efflux was initiated by sedimentation

at 600  $\times$  *g* and resuspension in rhodamine-free media, continuing with or without CsA or 1, 10, and 100  $\mu$ M concentration of the test compound. The efflux was carried out at 37° in 5% CO<sub>2</sub> for 60 min. At the end of both the accumulation and efflux periods, cells were sedimented, washed, placed on ice in Hanks' balanced salt solution with 10% fetal calf serum, and kept in the dark until flow cytometric analysis. As a precaution, the fluorescence was also determined for the highest concentration of each test compound in the absence of rhodamine 123. Samples were analyzed on a FACScan flow cytometer (Becton-Dickinson, San Jose, CA) equipped with a 488-nm argon laser. The fluorescence of rhodamine 123 was collected after a 530-nm band-pass filter. Samples were gated on forward scatter versus side scatter to exclude cell debris and clumps. A minimum of 6000 events were collected for each sample.

**Cytotoxicity assay.** Cells were seeded onto 96-well plates (2000 cells/well); 24 hr later, increasing doses of the test compounds were added in the presence or absence of 3  $\mu$ g/ml CsA. The cells were incubated for 4 days in the test compound before fixation in 10% trichloroacetic acid and staining with 0.4% sulforhodamine B in 1% acetic acid (27). The bound dye was solubilized in 100–200  $\mu$ l of 10 mM unbuffered Tris solution, and absorbance was determined at the wavelength of 540 nm in a microplate reader (BioRad, Richmond, CA).

**Azidopine labeling.** Plasma membranes from SW620 Ad300 cells were prepared and photolabeled with 1  $\mu$ Ci of <sup>3</sup>H-azidopine as previously described (28). Then, 100  $\mu$ g of total membranes were incubated for 15 min with <sup>3</sup>H-azidopine in the presence or absence of the test compound. The membranes were photolabeled with a UV lamp (General Electric F15T8) on ice for 15 min. Laemmli's buffer was added, and the samples were run on a 7.5% sodium dodecyl sulfate-polyacrylamide gel. After gel enhancement with Enlightening (New England Nuclear Research Products, Boston, MA), the gel was dried and prepared for autoradiography.

**Drug accumulation.** Drug accumulation studies were performed as previously reported (29). Briefly, 3.5  $\times$  10<sup>5</sup> cells were plated into each well of a six-well plate. SW620 Ad300 cells were rinsed and incubated with assay medium before initiation of the drug accumulation assay that was performed with 2  $\times$  10<sup>6</sup> dpm/well [<sup>3</sup>H]vinblastine.

**ATPase assay.** The ATPase activity of the isolated *Sf9* cell membranes (11) was estimated by measuring inorganic phosphate liberation. The ATPase activity of the membranes was determined in the presence of the various test compounds and compared with the activity induced by 10  $\mu$ M verapamil, as previously described (30).

**Kinetic studies.** Kinetic parameters were calculated based on the effect of the 18 test compounds on [<sup>3</sup>H]daunorubicin accumulation in P388/Adr multidrug-resistant lymphoma cells, as previously described (31). The  $K_i$  value was obtained by fitting the data to a modified form of the Michaelis-Menten equation:

$$D_i = D_o + \frac{(D_{inf} - D_o) \times C}{C + K_i \left( \frac{D_{inf}}{D_o} \right)}$$

where  $D_i$  is the amount of daunorubicin within the cells at the steady state (1-hr incubation at 37° with 2 nM daunorubicin) in the presence of a concentration  $C$  of the reverser,  $D_o$  is the amount in the absence of the reverser, and  $D_{inf}$  is the computed amount within the cells at an infinite concentration of the reverser.  $K_i$  is the derived value of the Michaelis constant that gives the amount of the reverser required to block one half of the pumping ability of Pgp. This equation is derived in full in Lan *et al.* (31) and Ayesh *et al.* (32), in which the complete details of the experimental methods are described.

## Results

**Reversal of cytotoxicity in the presence or absence of CsA.** To increase our understanding of the interaction of

Pgp with its substrates and antagonists, we studied compounds selected from the National Cancer Institute Drug Screen database as described in Experimental Procedures. These compounds included 120 individual structures and 47 analogues of NSC 667739, which was identified as a Pgp antagonist in preliminary studies. Included in the 120 compounds were four well-known Pgp substrates (vinblastine, doxorubicin, colchicine, and paclitaxel) and three well-known Pgp antagonists (CsA, PSC 833, and verapamil).

One hallmark of a Pgp substrate is the potentiation of its cytotoxicity by a known Pgp antagonist, such as CsA. Thus, the cytotoxicity of each of the 167 compounds was tested in the absence or presence of CsA in SW620 Ad300 cells. SW620 Ad300 cells were chosen as a well-characterized multidrug-resistant cell line in which Pgp overexpression is the exclusive mechanism of acquired resistance (25). Cells were treated with increasing concentrations of each test compound with or without 3  $\mu\text{g/ml}$  CsA. The DMF was defined as the ratio between the  $\text{IC}_{50}$  in the absence and the presence of CsA. The effect of the addition of CsA varied widely; the potency of some compounds (e.g., NSC 38270, 630176, and 359449) was enhanced by the addition of CsA, whereas for other compounds (e.g., NSC 68075, 665333, and 667739), CsA had minimal or no impact. Pgp "substrates" were prospectively defined as compounds with a DMF of  $>4$ , based on the premise that a 4-fold sensitization by CsA in the SW620 Ad300 cells indicates reversal of transport by Pgp. According to this criterion, 42 compounds were defined as substrates. The results of 18 compounds chosen for further analysis as

described below are shown in Table 1; 10 test compounds meeting the criterion as a substrate, along with the results of eight compounds that did not meet the criterion, are shown. These results are compared with the results obtained with the well-known Pgp substrates and antagonists. For CsA, PSC 833, and verapamil and the eight compounds in Table 1 with a DMF of  $<4$ , independent cytotoxicity studies comparing SW620 parental and SW620 Ad300 resistant cells confirmed the lack of cross-resistance (Pgp-mediated), which was implicit in the failure to be sensitized by the addition of CsA. The degree of sensitization observed for the substrates was also confirmed by evaluation of the  $\text{IC}_{50}$  value in SW620 parental cells (Table 1).

#### Inhibition of rhodamine efflux in SW620 Ad300 cells.

Pgp antagonists interfere with rhodamine efflux and thus increase rhodamine 123 accumulation (23, 33–35). We performed FACS analysis to determine which of the 167 compounds were able to inhibit rhodamine efflux. Cells were incubated in rhodamine in the presence or absence of the test compound, washed, and then incubated for 30 min in rhodamine-free medium, continuing in the presence or absence of the test compound. The amount of rhodamine remaining in the cells after the efflux period was quantified by flow cytometric analysis. Fig. 1 depicts the histogram for NSC 667739 as an example of the assay used for definition of Pgp antagonists. The "channel shift" value chosen as an index of Pgp antagonism is calculated by subtracting the mean channel number of rhodamine 123 fluorescence in control cells from the mean channel number of rhodamine 123 fluorescence in

TABLE 1  
Results of cytotoxicity assays for 18 compounds selected from the National Cancer Institute Drug Screen Repository

NSC number (class) <sup>a</sup>	SW620 $\text{IC}_{50}$ $\mu\text{g/ml}$	SW620 Ad300		DMF <sup>b</sup>
		$\text{IC}_{50}$	$\text{IC}_{50} + \text{CsA}$	
		$\mu\text{g/ml}$	$\mu\text{g/ml}$	
38270 (S)	0.002	30	0.0037	8000
328426 (S)	0.000001	3	0.0025	1200
339281 (S)	1.3	200	3	66.6
359449 (S)	0.7	150	0.100	1500
630176 (S)	0.002	1.5	0.00015	10000
633043 (S)	1.5	60	0.500	120
640085 (S)	0.2	60	0.60	100
666490 (S)	0.2	150	0.100	1500
68075 (A)	8.5	10	10	1
665333 (A)	5.5	10	10	1
667739 (A)	2.8	4	10	0.4
676590 (A)	26	20	10	2
676591 (A)	20	5	5	1
676597 (A)	2.4	1	2	0.5
676599 (A)	33	70	41	1.7
676600 (A)	N.D.	10	25	0.4
676605 (O)	80	30	5	6
668360 (O)	1.5	1	0.071	14
Vinblastine		0.04	0.00011	351
Doxorubicin		1.36	0.0056	241
Paclitaxel		0.220	0.0022	100
Colchicine		0.100	0.006	16.6
CsA <sup>c</sup>	7	23		3.3
PSC 833 <sup>c</sup>	7	21		3
Verapamil <sup>c</sup>	60	90		1.5

<sup>a</sup> Classification determined by assays in Tables 1 and 2: S, substrate; A, antagonist; and O, compounds in the overlap group.

<sup>b</sup>  $\text{DMF} = \text{IC}_{50}/(\text{IC}_{50} + \text{CsA})$  in SW620 cells.

<sup>c</sup> Cytotoxicity for CsA, verapamil, and PSC 833 has been tested, and the DMF determined through comparison of  $\text{IC}_{50}$  value of SW620 Ad300 cells with that of the parental SW620 cells.

N.D., not determined.

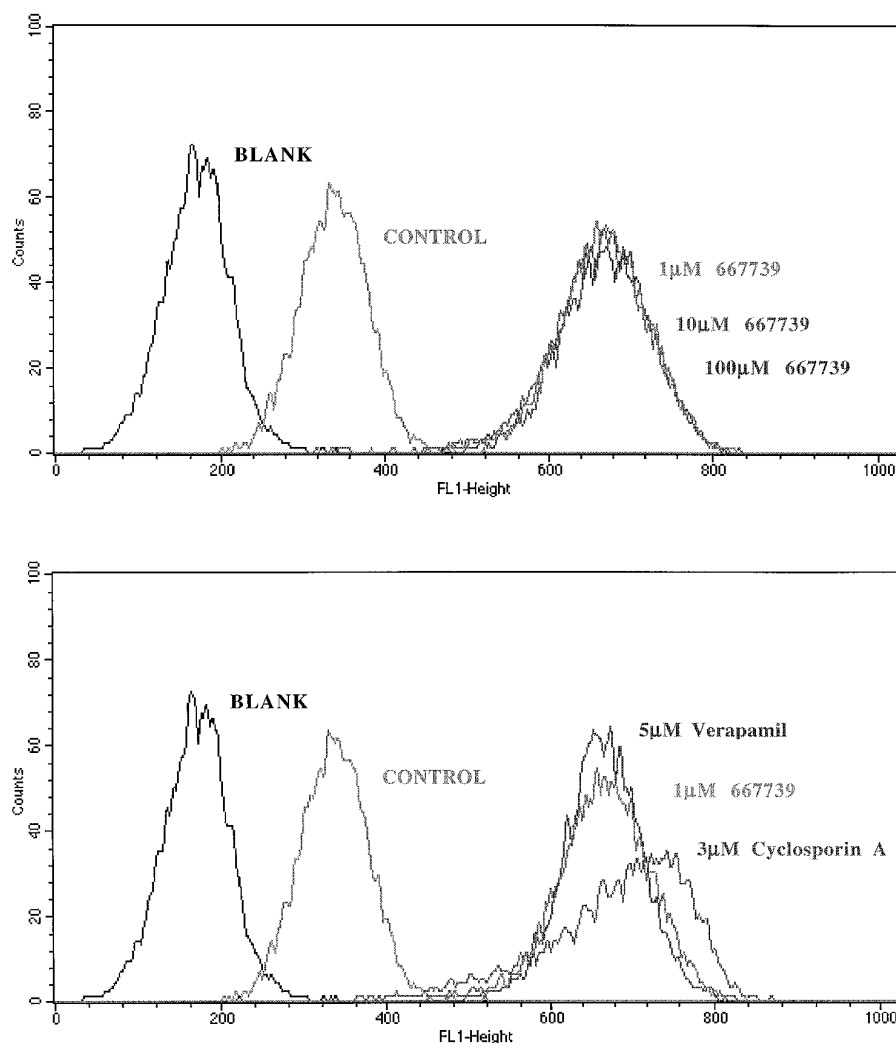


**Fig. 1.** Example of rhodamine efflux assay in SW620 Ad300 cells: NSC 667739. SW620 Ad300 cells were trypsinized and aliquoted in 100  $\mu$ l in 96-well plates. Cells were incubated in rhodamine-containing media for 30 min in the absence or presence of NSC 667739, verapamil, or CsA. The cells were then washed and allowed to efflux in rhodamine-free media, continuing in the absence or presence of modulator for 60 min. The amount of rhodamine still present in the cells at the end of the efflux period was measured. *BLANK*, autofluorescence of cells in rhodamine-free media. *CONTROL*, fluorescence intensity at the end of the efflux period in the absence of added compound or modulator. The mean channel shift is obtained by subtracting the control rhodamine fluorescence intensity (channel number) from the rhodamine fluorescence intensity (channel number) observed in the presence of compound. *Top*, comparable fluorescence intensity is obtained in the presence of three different concentrations of NSC 667739 (1, 10, and 100  $\mu$ M). *Bottom*, comparison of the change in rhodamine fluorescence intensity induced by NSC 667739 (1  $\mu$ M) and two known Pgp antagonists, verapamil (5  $\mu$ M) and CsA (3  $\mu$ g/ml).

the presence of the test compound. The definition of an “antagonist” was set prospectively as a test compound capable of shifting the fluorescence intensity of  $\geq 150$  channels at concentrations of either 1, 10, or 100  $\mu$ M. The 150-channel shift represents a 4-fold increase in rhodamine accumulation. By this criterion, 49 test compounds were identified as antagonists. Seven of these had also been identified as substrates by the cytotoxicity assay with CsA described above; these were labeled as an “overlap” (O) group. Table 2 shows the results with eight compounds meeting only the criterion of an antagonist (A), along with the results with eight compounds that met only the criterion for a substrate (S), and the results with two compounds that met both criteria (O). One of the test compounds chosen by COMPARE for its high correlation with *d*-verapamil (0.797), NSC 68075, or thaliblastine was identified as an antagonist in the rhodamine assay and subsequently found to have been previously reported as a Pgp antagonist (36).

**Compounds cluster into two groups.** Thus, of the 167 compounds tested in the cytotoxicity assay and the rhodamine efflux assay (Fig. 1), 84 met at least one criterion. Of the 84, seven satisfied both criteria, whereas 35 were identified as substrates only and 42 were classified as antagonists only. Fig. 2 presents a scatterplot of the data obtained on the 84 test compounds that met either criterion defining an inter-

action with Pgp. Included in the 84 were 21 of the 47 analogues of NSC 667739. Among these 21 were 17 antagonists, two substrates, and two classified as overlap compounds. The 83 test compounds that did not satisfy either criterion included eight with high levels of autofluorescence and 13 that were nontoxic, so they could not be classified. Seven of the eight with high autofluorescence and three of the 13 nontoxic compounds were derived from the NSC 667739 analogue series. The remaining 62 compounds (including 16 of the analogues) did not meet the criterion of a substrate or an antagonist and were thus thought to have no interaction with Pgp. The maximum channel shift obtained from each of the 84 compounds meeting either criterion is plotted on the *x*-axis, while the DMF in the presence of CsA is plotted on the *y*-axis. These compounds cluster into two large groups; these groups are statistically significantly different for both DMF ( $p = 0.03$ , Student's *t* test) and channel shift ( $p < 0.002$ , Student's *t* test).

**Eighteen test compounds were chosen for further analysis.** The 18 test compounds presented in Tables 1 and 2 were a subgroup chosen for further studies. They were selected from among the 84 compounds identified as substrates, antagonists, or both (overlap). The substrates chosen had high levels of reversal (8 compounds with a DMF of  $> 50$ ), whereas the antagonists were potent at the lower concentra-



TABLE 2

**Results of rhodamine 123 efflux assays for 18 compounds selected from National Cancer Institute Drug Screen Repository**

	Mean channel shift of rhodamine fluorescence in SW620 Ad300 cells <sup>a</sup>		
	1 $\mu$ M	10 $\mu$ M	100 $\mu$ M
NSC number (class) <sup>b</sup>			
38270 (S)	44	38	0
328426 (S)	0	0	283
339281 (S)	0	25	c
359449 (S)	0	29	128
630176 (S)	36	32	35
633043 (S)	0	0	0
640085 (S)	11	18	19
666490 (S)	0	0	0
68075 (A)	55	326	331
665333 (A)	165	391	357
667739 (A)	362	360	362
676590 (A)	48	163	419
676591 (A)	144	348	420
676597 (A)	219	438	447
676599 (A)	0	188	452
676600 (A)	186	205	307
676605 (O)	51	281	304
668360 (O)	N.D.	192	415
Vinblastine	0	79	516
Doxorubicin	0	0	29
Paclitaxel	189	284	291
Colchicine	11	3	0
CsA	202	381	373
PSC 833	330	362	401
Verapamil	75	316	407

<sup>a</sup> Difference in rhodamine fluorescence intensity in the presence and absence of 1, 10, and 100  $\mu$ M of the tested drug (mean channel shift). 0, Absence of detectable effect.

<sup>b</sup> Classification determined by assays in Tables 1 and 2: S, substrate; A, antagonist; and O, compounds in overlap group.

<sup>c</sup> Autofluorescence is too high at 100  $\mu$ M to be reliable.

N.D., not determined.

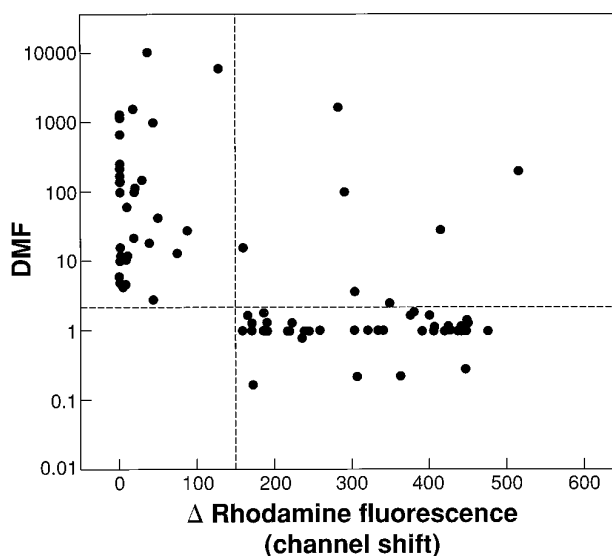


**Fig. 2.** Scatterplot of calculated DMF and channel shift values. Statistical evaluation performed on the 84 compounds showed that Pgp substrates and antagonists form two groups that are significantly different.

tion tested (8 compounds inducing a shift at 10  $\mu$ M of >150 channels of rhodamine fluorescence). Two compounds chosen met both criteria. The group of antagonists includes NSC 667739, the most potent antagonist found, which was able to

inhibit rhodamine efflux at 1  $\mu$ M, the lowest concentration tested. Six analogues of NSC 667739 (676590, 676591, 676597, 676599, 676600, 676605) were included. The structures of these 18 compounds are shown in Fig. 3.

**Modulation of [<sup>3</sup>H]vinblastine accumulation.** The results obtained with the rhodamine efflux assay were confirmed by examining the effect of the eight substrates from Tables 1 and 2 on the accumulation of [<sup>3</sup>H]vinblastine in SW620 Ad300 cells. These results were compared with those observed with three compounds from the antagonist subgroup and two compounds from the overlap subgroup. Fig. 4 shows the results of the [<sup>3</sup>H]vinblastine accumulation carried out in the presence of a 10- $\mu$ M concentration of each of the test compounds compared with the effect of a known Pgp antagonist, PSC 833 (3  $\mu$ g/ml). Vinblastine accumulation in the absence of other compounds is arbitrarily set at 100%. The test compounds identified as substrates had little impact on [<sup>3</sup>H]vinblastine accumulation. In contrast, the test compounds identified as antagonists increased vinblastine accumulation by 7.5–8-fold compared with a 10-fold increase observed with PSC 833.

**Kinetic studies.** As previously reported, it is possible to analyze the kinetic parameters for antagonism of Pgp function (31). We measured the kinetic parameters of the 18 selected compounds by determining their effects on [<sup>3</sup>H]daunorubicin accumulation in P388/Adr cells and calculated a  $K_i$  value for Pgp inhibition. The  $K_i$  value for reversal ( $K_{i \text{ reversal}}$ ) defines the concentration of antagonist at which half of the Pgp-mediated transport is blocked. The  $K_i$  value was determined by fitting the data to a modified Michaelis-Menten equation as described in Experimental Procedures. Table 3 shows the calculated  $K_i$  value for each of the 18 test compounds. A significant correlation was found between the data shown in Table 2 and the  $K_i$  value ( $p = 0.0003$ ). The substrates NSC 38270, 359449, 630176, 633043, 640085, and 666490 have a  $K_i$  value of >100, whereas the antagonists NSC 68075, 665333, 676591, 676597, and 676600 have a  $K_i$  value of <1.

**Inhibition of <sup>3</sup>H-azidopine photolabeling of Pgp by selected antagonists and substrates.** The ability to inhibit photoaffinity labeling of Pgp by the compound azidopine has frequently been used as an indicator of whether a particular compound interacts with Pgp (37, 38). Specifically, it is believed that compounds that block photolabeling do so by competing for a common binding site on Pgp (39). To determine whether differences in azidopine competition could be found between the substrate and antagonist groups, labeling experiments were performed with the group of 18 selected compounds. Fig. 5 shows the densitometric analysis of the inhibition of <sup>3</sup>H-azidopine labeling in the presence of a 200- $\mu$ M concentration of each test compound. Although all of the test compounds were able to compete <sup>3</sup>H-azidopine labeling to some extent, we observed a range of inhibition, suggesting binding to different Pgp sites or differing affinities for the azidopine binding site.

**Drug-stimulated ATPase activity.** As previously reported, Pgp exhibits drug-dependent ATPase activity, which is consistent with coupling of drug transport to ATP hydrolysis (11, 30, 40). Seventeen of the 18 compounds were examined for their ability to stimulate ATPase activity in membranes obtained from Sf9 cells infected with a recombinant baculovirus containing the MDR-1 cDNA. Cell membranes

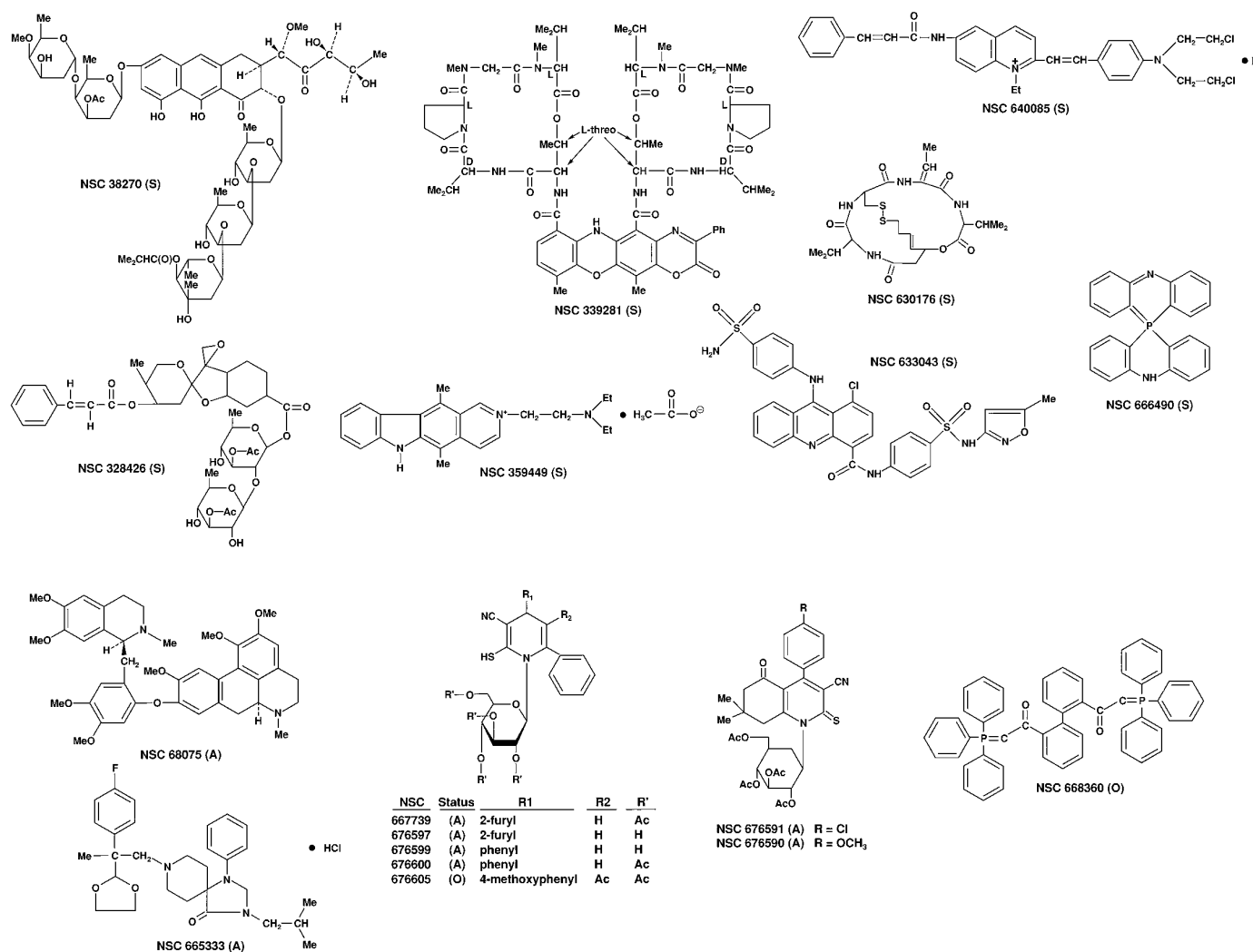


**Fig. 3.** Structures of the 18 selected compounds, including 6 analogues of NSC 667739 (676590, 676591, 676597, 676599, 676600, and 676605).

were obtained as described, and ATP hydrolysis was assayed in the presence of 10  $\mu$ M verapamil or 10- $\mu$ M concentrations of each test compound (30). Fig. 6 shows the ATPase activity, measured as inorganic phosphate hydrolyzed from 5 mM Mg<sup>+</sup>ATP. Substrates NSC 328426 and 633043 and antagonists NSC 676597 and 676599 stimulated the ATPase activity. However, substrates such as NSC 38270 and 630176 and antagonists such as NSC 68075 and 667739 had a negligible effect on ATPase activity.

**Correlation coefficients among the studied parameters.** Table 4 shows the results of pairwise correlations of the parameters measured and described above: DMF, channel shift value with 10- $\mu$ M concentrations of each test compound,  $K_i$  reversal, increase in vinblastine accumulation, induction of ATPase activity, and inhibition of azidopine labeling. Pearson correlation coefficients were calculated for each pair. Significant inverse correlations were observed between the DMF and both the channel shift value (−0.847) and the increase in vinblastine accumulation (−0.874), and a direct correlation was noted for the DMF and the calculated  $K_i$  value (0.822). An inverse correlation was noted for the channel shift measurement and the calculated  $K_i$  value (−0.744), whereas a direct correlation was noted between the channel shift value and the increase in vinblastine accumulation

(0.899). No significant correlation could be found between the inhibition of azidopine binding and stimulation of ATPase activity and any of the other parameters.

**Properties of test compounds.** In a previous study, we calculated an average molecular weight of 325 for the 452,084 compounds in the National Cancer Institute chemical database with defined molecular weights (23). In the current study, the 84 compounds that met the criterion of either a substrate or of an antagonist had an average molecular weight of 602, which is 1.9 times the average in the National Cancer Institute chemical database. This group of compounds was divided into three groups: the 35 that were substrates only had an average molecular weight of 636, which is 2.0 times the National Cancer Institute average; the 42 that were antagonists only had an average molecular weight of 558, which is 1.7 times the National Cancer Institute average; and the seven that were both substrates and antagonists had an average molecular weight of 739, which is 2.3 times the National Cancer Institute average. Compounds of high and low molecular weight could be found in every group. The molecular weight ranges were 326–1372, 322–1214, and 549–909 for substrates, antagonists, and overlap compounds, respectively. The percentage of compounds with at least one positively charged atom at physiological pH was

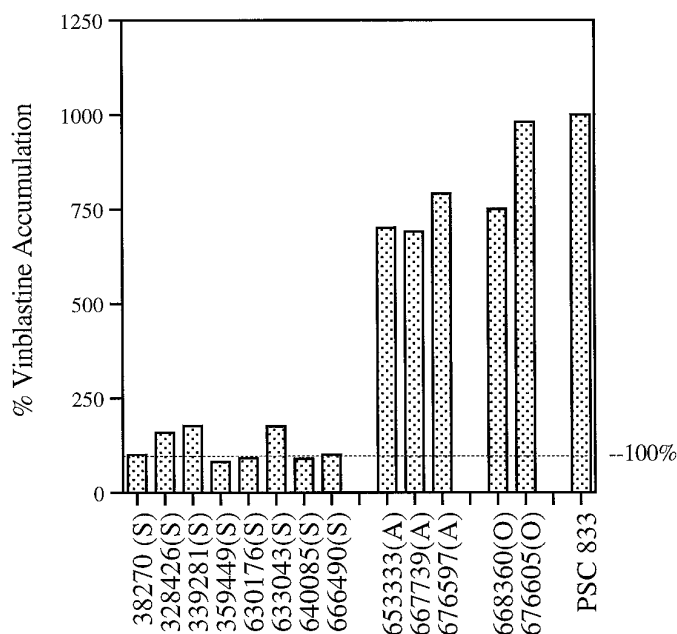


**Fig. 4.** [ $^3\text{H}$ ]Vinblastine accumulation in SW620 Ad300 cells. Accumulation of 14 nM [ $^3\text{H}$ ]vinblastine in the absence or presence of 10  $\mu\text{M}$  concentration of the selected compounds is shown. In this experiment, the accumulation in the SW620 Ad300 cells in the absence of added compound is assigned a value of 100%.

TABLE 3

**$K_{\text{reversal}}$  values for substrates and antagonists**

$K_{\text{reversal}}$  is the concentration ( $\mu\text{M}$ ) at which half of the Pgp-mediated transport is blocked.

NSC	$K_{\text{reversal}}$
<b>Substrate</b>	
38270 (S)	>100
328426 (S)	5.44
339281 (S)	2.55
359449 (S)	>100
630176 (S)	>100
633043 (S)	>100
640085 (S)	>100
666490 (S)	>100
<b>Antagonist</b>	
68075 (A)	0.37
665333 (A)	0.28
667739 (A)	5.13
676590 (A)	1.42
676591 (A)	0.28
676597 (A)	0.62
676599 (A)	2.18
676600 (A)	0.06
<b>Overlap</b>	
676605 (O)	0.48
668360 (O)	0.25

calculated: 42% of all 84 compounds, 50% of substrates, 40% of antagonists, and 29% of compounds in the overlap group. Two anionic compounds (2.4%) were observed in the group of 84 compounds.

The 167 compounds included 47 analogues of NSC 667739. This provided the opportunity to examine the effect of a wide range of structural modifications on Pgp antagonism. The analogue series is composed of 3-cyanopyridine-2-thiones and 2-thiol-3-cyano-1,4-dihydropyridines as *N*-glucosides and *N*-galactosides, respectively. Of these, 17 were antagonists, two were substrates, and two were classified as overlap com-

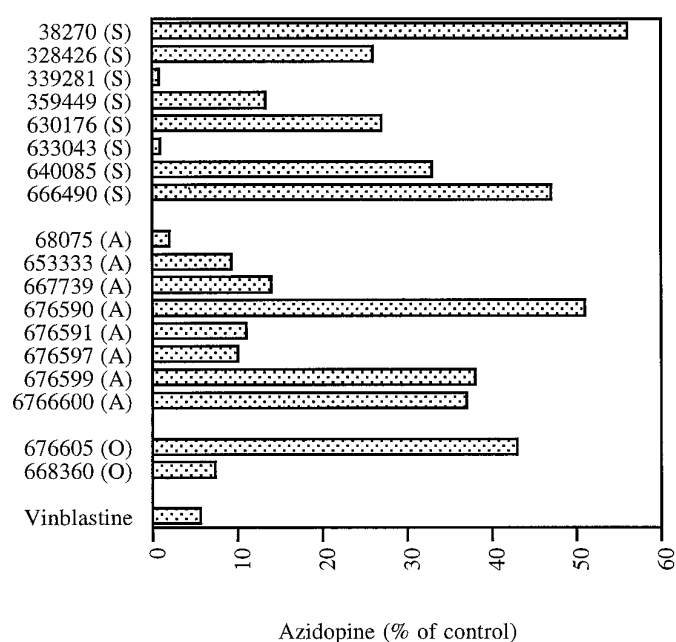


**Fig. 5.** [ $^3\text{H}$ ]Azidopine photoaffinity labeling in SW620 Ad300 cells. Total cell membranes were prepared from SW620 Ad300 cells. Cell membranes (100  $\mu\text{g}$ ) were incubated with 1  $\mu\text{Ci}$  of [ $^3\text{H}$ ]azidopine in the presence or absence of 200  $\mu\text{M}$  concentration of the agents for 30 min. After cross-linking, membranes were resolved on a sodium dodecyl sulfate-7.5% polyacrylamide gel. Results are from the densitometric analysis of the resulting autoradiogram.

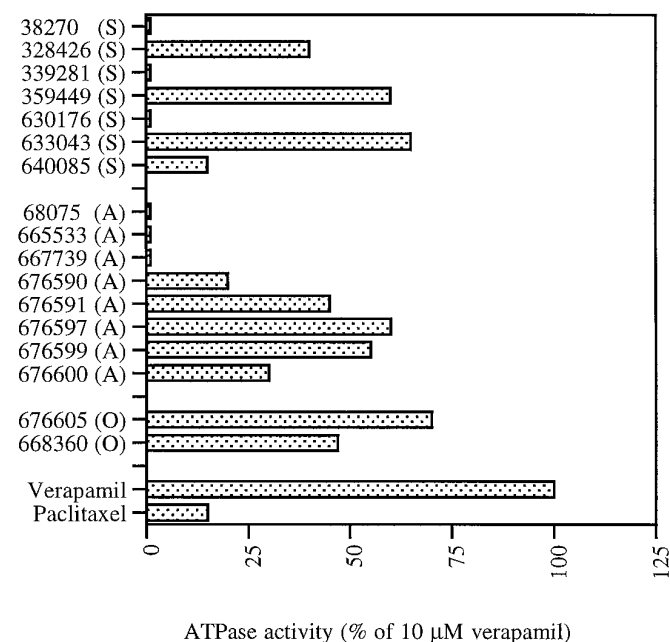


**Fig. 6.** ATPase activity in membranes from Sf9 cells infected with a recombinant baculovirus containing the MDR-1 cDNA. Cell membranes were incubated in the presence of 10  $\mu\text{M}$  verapamil and 10  $\mu\text{M}$  concentration of each tested compound.

pounds. The remaining 26 were either unclassifiable or had no interaction with Pgp. The structures of the 21 compounds that could be classified were examined. Only the blockers were present in sufficient numbers to make structure-based observations about them. The structural requirements for Pgp-blocking activity within this particular group of glyco-

TABLE 4  
Pearson correlation coefficients of tested parameters

Parameter	Parameter	r
DMF	Channel shift	-0.847
	Vinblastine accumulation	-0.874
	$K_i$ reversal	+0.822
	Azidopine labeling	+0.261
	ATPase induction	-0.095
Channel shift	Vinblastine accumulation	+0.899
	$K_i$ reversal	-0.744
	Azidopine labeling	-0.291
	ATPase induction	+0.039
Vinblastine accumulation	$K_i$ reversal	-0.852
	Azidopine labeling	-0.054
	ATPase induction	+0.240
	Azidopine labeling	+0.220
$K_i$ reversal	ATPase induction	-0.095
	ATPase induction	-0.034

sides are quite broad. Effective blockers were found with the pyridine-2-thione substructure and with the dihydropyridine substructure, as the galactosides and as the glucosides, as the peracylated sugars or the nonacylated sugars. The 4 and 6 positions could be alkyl or aryl substituted. The 5 position could be alkyl, aryl, acyl, or hydrogen. The two substrates were both glucosides and were pyridine-2-thiones. The two overlap compounds were both glucosides; one was a dihydropyridine and the other was a pyridine-2-thione.

## Discussion

The mechanism by which Pgp binds and transports a broad array of compounds is still largely unknown. To gain further insight into this mechanism, we classified 84 compounds from the National Cancer Institute Drug Screen database as Pgp substrates and/or antagonists. Thirty-five compounds were classified as substrates only (increased cytotoxicity in the presence of CsA), and 42 were identified as antagonists only (ability to inhibit rhodamine efflux). Seven compounds were designated "overlap" because they shared both features. For further study, we concentrated on a subset of 18 compounds composed of the eight most potent substrates, the eight most potent antagonists; and two of the seven compounds in the overlap group. Vinblastine accumulation studies and kinetic studies succeeded in discriminating substrates and antagonists, whereas induction of ATPase activity and inhibition of azidopine labeling failed to distinguish the groups. These variable interactions with the Pgp molecule support a model of Pgp in which there is a region of interaction rather than one or two simple binding sites.

Extensive published evidence suggests that multiple sites in Pgp participate in the interaction with compounds. Mutations at specific sites in virtually all of the transmembrane regions of Pgp have had functional consequences; affecting different compounds differently either in conferring resistance or in antagonistic potential (10, 12, 16, 41, 42). Loo and Clarke (43) demonstrated multiple mutations in transmembrane regions of Pgp that led to altered substrate specificity. For example, mutation of Phe335 to alanine or serine resulted in loss of colchicine and doxorubicin resistance with preserved actinomycin D resistance (13, 14). Similar results were observed with mutation of Gly341 to valine (15).

The current data suggest two nonoverlapping interactions of molecules with Pgp, one classified as "substrate" and the

other classified as "antagonist." Compounds in the substrate group were characterized by a  $\geq 4$ -fold increase in cytotoxicity in multidrug-resistant cells. Unlike the classic paradigm in which a Pgp substrate is also an antagonist if administered in sufficiently high concentrations (8, 9), some of these substrates failed to increase rhodamine or vinblastine accumulation, despite the 100  $\mu\text{M}$  concentration that was used. Compounds in the antagonist subgroup increased rhodamine and vinblastine accumulation and displayed  $<4$ -fold reversal of cytotoxicity by CsA, suggesting that they are poorly transported. These results extend previous work in our laboratory that suggested that increased transport of a substrate is associated with decreased antagonistic activity (20, 21). Drug accumulation studies confirmed indirectly that several of the known blockers are poorly transported by Pgp. Levels of verapamil, progesterone, tamoxifen, and forskolin in SW620 Ad300 multidrug-resistant cells were found to be 67%, 97%, 100%, and 112%, respectively, of those found in parental cells. In comparison, vinblastine accumulation was 12% of that in parental cells.<sup>1</sup> Although transport of these antagonists may be present to some extent, it is not sufficient to result in sensitization by CsA or in cross-resistance in multidrug-resistant cells. This is true for both the known antagonists and the new compounds identified by the National Cancer Institute Drug Screen. These results suggest that antagonism could result from a tighter binding to Pgp, associated with poor transport relative to substrates that have an efficient transport. Interestingly, compounds in the antagonist group are relatively less toxic than compounds in the substrate group, with a median  $\text{IC}_{50}$  value of 22.5  $\mu\text{M}$  for the antagonists compared with a median  $\text{IC}_{50}$  value of 0.175  $\mu\text{M}$  for the substrates.

These results agree with previous studies suggesting more than one type of interaction with Pgp. It has been reported that Pgp antagonists compose two groups: one transported and the other not transported (17–19, 44). Ayesch *et al.* (32) demonstrated competitive and noncompetitive kinetics for different modulators. Rao (11) described two classes of agents interacting with Pgp: one activating ATPase activity (implying transport) and the other failing to activate ATPase activity.

We next asked whether other assays could discriminate the two groups, giving insight into the mechanism underlying the different interactions with Pgp. Competition with azidopine for its binding site has been described for numerous Pgp substrates and antagonists (17, 18, 37–39). However, the inhibition of azidopine has not been clearly correlated with the ability of a compound to block drug transport (7, 18, 39). At 200  $\mu\text{M}$ , all of the tested compounds inhibited azidopine labeling, although the extent of inhibition varied. Lower concentrations in many cases demonstrated no inhibition of azidopine labeling, and 200  $\mu\text{M}$  was chosen to demonstrate some interaction for all the compounds. Inhibition of azidopine binding did not seem to correlate with the capacity of a compound to be either a substrate (DMF) or an antagonist (mean channel shift), with Pearson correlation coefficients of 0.261 and -0.291, respectively. In fact, two substrates with profound reversal of cytotoxicity by CsA (DMF  $> 1000$ ) are the weakest inhibitors of  $^3\text{H}$ -azidopine binding (NSC 38270 and 630176). Either these substrates bind Pgp in a site

<sup>1</sup> S. Scala, N. Akhmed, and S. E. Bates, unpublished observations.



different from that of azidopine or their affinity for the azidopine binding site is lower than that of azidopine itself. One extension of these findings is the conclusion that competition with azidopine binding is insufficient to determine the interaction and/or binding of a compound to Pgp.

Drug-induced increases in ATPase activity have been observed in several model systems, including both selected cells and cells transfected with *MDR-1* (30, 45, 46). Both substrates and antagonists induce the activity, including verapamil, trifluoperazine, rhodamine, progesterone, quinidine, vinblastine, and colchicine (11, 30, 40). However, Rao (11) recently described the failure of the antagonist CsA to activate the ATPase activity and its ability to inhibit ATPase activation by verapamil and vinblastine. Similar results were observed in the 18 compounds selected for a more detailed analysis. There was no significant correlation between ATPase activity and whether a compound was a substrate (DMF) or an antagonist (mean channel shift), with Pearson correlation coefficients of  $-0.095$  and  $+0.039$ , respectively. Three substrates with a high DMF and two of the most potent antagonists failed to stimulate the ATPase activity.

The test compounds were also not distinguishable by molecular weight or charge at physiological pH. In previous studies, hundreds of potential new Pgp substrates were identified, and dozens were confirmed among the 40,000 compounds in the National Cancer Institute Drug Screen database (23, 24). Examination of the top 100 correlating compounds revealed that the average molecular weight of the neutral molecules was 861; whereas the average molecular weight of compounds that were cationic at physiological pH was 517 (23). In the current study, the average molecular weight for the substrates was 636, whereas the average molecular weight for the antagonists was 558. In all of the subsets, the molecular weight is higher than that calculated for the "average" chemical compound, which was calculated as 325 on the basis of the 452,084 compounds in the National Cancer Institute chemical database. This is in agreement with previous observations that Pgp substrates tend to be compounds of large molecular weight.

Taken together, analysis of 167 compounds demonstrated that compounds that interact with Pgp, both substrates and antagonists, form two distinctive groups. Although two separate binding sites could be invoked to explain the data, it seems more likely that multiple regions in Pgp participate in transport, as suggested by site-directed mutagenesis studies. Our findings imply that the antagonists bind to Pgp but failing transport, prevent the transport of other agents, and that substrates, in being transported, do not block the transport of other substrates. It is clear from the variability in inhibition of azidopine binding and induction of ATPase activity within the two groups that there is a complexity of interaction between Pgp and different compounds.

#### Acknowledgments

The authors thank Dalia Cohen and Ahmad Safa for helpful discussions; Jill Johnson for distribution of the National Cancer Institute compounds; and Tito Fojo, Ed Sausville, and Susan Mertins for careful reading of the manuscript.

#### References

- Gottesman, M. M., and I. Pastan. Biochemistry of multidrug resistance mediated by the multidrug transporter. *Annu. Rev. Biochem.* **62**:385–427 (1993).
- Fojo, A. T., K. Ueda, D. J. Slamon, D. G. Poplack, M. M. Gottesman, and I. Pastan. Expression of a multidrug resistance gene in human tumors and tissues. *Proc. Natl. Acad. Sci. USA* **84**:265–269 (1987).
- Eytan, G., R. Borgnia, R. Regev, and Y. Assaraf. Transport of polypeptide ionophores into proteoliposomes reconstituted with rat liver P-glycoprotein. *J. Biol. Chem.* **269**:26058–26065 (1994).
- Raymond, M., P. Gros, M. Whiteway, and D. Thomas. Functional complementation of yeast *ste6* by a mammalian multidrug resistance *mdr* gene. *Science (Washington D. C.)* **232**:232–234 (1992).
- Deverson, E., I. Gow, W. Coadwell, J. Monaco, G. Butcher, and J. Howard. MHC class II region encoding proteins related to the multidrug resistance family of transmembrane transporters. *Nature (Lond.)* **348**:738–741 (1990).
- Masci, A., S. Scala, L. Racioppi, and S. Zappacosta. Cell surface expression of Major Histocompatibility class I antigens is modulated by the P-glycoprotein transporter. *Hum. Immunol.* **42**:245–253 (1995).
- Sharom, G., G. Diodato, X. Yu, and K. Ashbourne. Interactions of the P-glycoprotein multidrug transporter with peptides and ionophores. *J. Biol. Chem.* **270**:10334–10341 (1995).
- Hait, W., and D. Aftab. Rational design and pre-clinical pharmacology of drugs for reversing multidrug resistance. *Biochem. Pharmacol.* **43**:103–107 (1992).
- Ford, J., and W. Hait. Pharmacologic circumvention of multidrug resistance. *Cytotech.* **12**:171–212 (1993).
- Cardarelli, C., I. Aksentijevich, I. Pastan, and M. Gottesman. Differential effects of P-glycoprotein inhibitors on NIH3T3 cells transfected with wild type (G185) or mutant (V185) multidrug transporter. *Cancer Res.* **55**:1086–1091 (1995).
- Rao, U. Mutation of glycine 185 to valine alters the ATPase function of the human P-glycoprotein expressed in Sf9 cells. *J. Biol. Chem.* **270**:6686–6690 (1995).
- Dhir, R., K. Grizzuti, S. Kajiji, and P. Gros. Modulatory effects on substrate specificity of independent mutations at the Ser<sup>939/941</sup> position in predicted transmembrane domain 11 of P-glycoproteins. *Biochemistry* **32**:9492–9497 (1993).
- Loo, T. W., and D. M. Clarke. Functional consequences of phenylalanine mutations in the predicted transmembrane domain of P-glycoprotein. *J. Biol. Chem.* **268**:19965–19972 (1993).
- Loo, T. W., and D. M. Clarke. Functional consequences of proline mutations in the predicted transmembrane domain of P-glycoprotein. *J. Biol. Chem.* **268**:3143–3149 (1993).
- Loo, T. W., and D. M. Clarke. Mutations to amino acids located in predicted transmembrane segment 6 (TM6) modulate the activity and substrate specificity of human P-glycoprotein. *Biochemistry* **33**:14049–14057 (1994).
- Kajiji, S., K. Dreslin, K. Grizzuti, and P. Gros. Structurally distinct MDR modulators show specific patterns of reversal against P-glycoproteins bearing unique mutations at serine<sup>939/941</sup>. *Biochemistry* **33**:5041–5048 (1994).
- Tamai, I., and A. R. Safa. Azidopine noncompetitively interacts with vinblastine and cyclosporin A binding to P-glycoprotein in multidrug resistant cells. *J. Biol. Chem.* **266**:16796–16800 (1991).
- Tamai, I., and A. R. Safa. Competitive interaction of cyclosporins with the vinca alkaloid-binding site of P-glycoprotein in multidrug resistant cells. *J. Biol. Chem.* **271**:16509–16513 (1996).
- Saeki, T., K. Ueda, Y. Tanigawara, R. Hori, and T. Komano. P-glycoprotein mediated transcellular transport of MDR-reversing agents. *FEBS Lett.* **324**:99–102 (1993).
- Bates, S. E., J. S. Lee, B. Dickstein, M. Spolyar, and A. T. Fojo. Differential modulation of P-glycoprotein transport by protein kinase inhibition. *Biochemistry* **32**:9156–9164 (1993).
- Barnes, K. M., B. Dickstein, Jr., G. B. Cutler, T. Fojo, and S. E. Bates. Steroid transport, accumulation, and antagonism of P-glycoprotein in multidrug-resistant cells. *Biochemistry* **35**:4820–4827 (1996).
- Paull, K. D., R. H. Shoemaker, L. Hodes, A. Monks, D. A. Scudiero, L. Rubinstein, J. Plowman, and M. R. Boyd. Display and analysis of patterns of differential activity of drugs against human tumor cell lines: development of mean graph and COMPARE algorithm. *J. Natl. Cancer Inst.* **81**:1088–1092 (1989).
- Lee, J. S., K. Paull, M. Alvarez, C. Hose, A. Monks, M. Grever, A. T. Fojo, and S. E. Bates. Rhodamine efflux patterns predict P-glycoprotein substrates in the National Cancer Institute Drug Screen. *Mol. Pharmacol.* **46**:627–638 (1994).
- Alvarez, M., K. Paull, A. Monks, C. Hose, J. S. Lee, J. Weinstein, M. Grever, S. Bates, and T. Fojo. Generation of a drug resistance profile by quantitation of *mdr-1*/P-glycoprotein in the cell lines of the National Cancer Institute Anticancer Drug Screen. *J. Clin. Invest.* **95**:2205–2214 (1995).
- Lai, G.-M., Y.-N. Chen, L. A. Mickley, A. T. Fojo, and S. E. Bates. P-glycoprotein expression and schedule dependence of Adriamycin cytotoxicity in human colon carcinoma cell lines. *Int. J. Cancer* **49**:696–703 (1991).
- Paull, K. D., C. M. Lin, L. Malspeis, and E. Hamel. Identification of novel antimitotic agents acting at the tubulin level by computer-assisted evaluation of differential cytotoxicity data. *Cancer Res.* **52**:3892–3900 (1992).
- Skehan, P., R. Storeng, D. Scudiero, A. Monks, J. McMahon, D. Vistica, J. T. Warren, H. Bokesch, S. Kenney, and M. R. Boyd. New colorimetric

- cytotoxicity assay for anticancer-drug screening. *J. Natl. Cancer Inst.* **82**:1107–1112 (1990).
28. Bruggemann, E. P., U. A. Germann, M. M. Gottesman, and I. Pastan. Two different regions of phosphoglycoprotein are photoaffinity labeled by azidopine. *J. Biol. Chem.* **264**:15483–15488 (1989).
29. Fojo, A., S. Akiyama, M. M. Gottesman, and I. Pastan. Reduced drug accumulation in multiply drug-resistant human KB carcinoma cell lines. *Cancer Res.* **45**:3002–3007 (1985).
30. Sarkadi, B., E. Price, R. Boucher, U. Germann, and G. Scarborough. Expression of the human multidrug resistance cDNA in insect cells generates a high activity drug-stimulated ATPase. *J. Biol. Chem.* **267**:4854–4858 (1992).
31. Lan, L.-B., S. Ayesh, E. Lyubimov, I. Pashinsky, and W. D. Stein. Kinetic parameters for reversal of the multidrug resistant pump as measured for drug accumulation and cell killing. *Cancer Chemother. Pharmacol.* **38**: 181–190 (1966).
32. Ayesh, S., Y. Shao, and W. D. Stein. Cooperative, competitive, and non-competitive interactions between modulators of the multidrug resistance pump. *Biochim. Biophys. Acta* **1316**:8–18 (1996).
33. Ludescher, C., J. Thaler, D. Drach, J. Drach, M. Spitaler, C. Gattringer, H. Huber, and J. Hofmann. Detection of activity of P-glycoprotein in human tumour samples using rhodamine 123. *Br. J. Haematol.* **82**:161–168 (1992).
34. Chaudhary, P. M., and I. B. Roninson. Expression and activity of P-glycoprotein, a multidrug efflux pump, in human hematopoietic stem cells. *Cell* **66**:85–94 (1991).
35. Lampidis, T. J., S. D. Bernal, I. C. Summerhayes, and L. B. Chen. Selective toxicity of rhodamine 123 in carcinoma cells in vitro. *Cancer Res.* **43**:716–720 (1983).
36. Chen, G., and D. J. Waxman. Complete reversal by thaliblastine of 490-fold adriamycin resistance in multidrug-resistant (MDR) human breast cancer cells: evidence that multiple biochemical changes in MDR cells need not correspond to multiple functional determinants for drug resistance. *J. Pharmacol. Exp. Ther.* **274**:1271–1277 (1995).
37. Safa, A. R. Photoaffinity labeling of the multidrug-resistance-related P-glycoprotein with photoactive analogs of verapamil. *Proc. Natl. Acad. Sci. USA* **85**:7187–7191 (1988).
38. Safa, A. R., C. J. Glover, J. L. Sewell, M. Meyers, J. Biedler, and R. Felsted. Identification of the multidrug resistance-related membrane glycoprotein as an acceptor for calcium channel blockers. *J. Biol. Chem.* **262**:7884–7888 (1987).
39. Safa, A. Photoaffinity labeling of P-glycoprotein in multidrug resistant cells. *Cancer Invest.* **10**:295–305 (1992).
40. Urbatsch, I., M. K. Al-Shawi, and A. E. Senior. Characterization of the ATPase activity of the purified Chinese hamster P-glycoprotein. *Biochemistry* **33**:7069–7076 (1994).
41. Choi, K., C. J. Chen, M. Kriegler, and I. B. Roninson. An altered pattern of cross-resistance in multidrug resistant human cells results from spontaneous mutations in the *mdr-1* (P-glycoprotein) gene. *Cell* **53**:519–529 (1988).
42. Zhang, X., K. I. Collins, and L. M. Greenberger. Functional evidence that transmembrane 12 and the loop between transmembrane 11 and 12 form part of the drug binding domain in P-glycoprotein encoded by MDR1. *J. Biol. Chem.* **270**:5441–5448 (1995).
43. Loo, T. W., and D. M. Clarke. Functional consequences of glycine mutations in the predicted cytoplasmic loops of P-glycoprotein. *J. Biol. Chem.* **269**:7243–7248 (1994).
44. Archinal-Mattheis, A., R. W. Rzepka, T. Watanabe, N. Kokubu, Y. Itoh, N. J. Combates, K. W. Bair, and D. Cohen. Analysis of the interaction of SDZ PSC 833 ([3'-keto-Bmt1]-Val2-cyclosporin), a multidrug resistance modulator, with P-glycoprotein. *Oncol. Res.* **7**:603–610 (1995).
45. Al-Shawi, M. K., I. L. Urbatsch, and A. E. Senior. Covalent inhibitors of P-glycoprotein ATPase activity. *J. Biol. Chem.* **269**:8986–8992 (1994).
46. Sharom, F., X. Yu, and C. Doige. Functional reconstitution of drug transport and ATPase activity in proteoliposomes containing partially purified P-glycoprotein. *J. Biol. Chem.* **268**:24197–24202 (1993).

**Send reprint requests to:** Susan E. Bates, M.D., Bldg. 10/Rm. 12N226, NCI/NIH, 9000 Rockville Pike, Bethesda, MD 20892. E-mail: [seabates@helix.nih.gov](mailto:seabates@helix.nih.gov)